# Distributed Consensus-Based Control of Multiple DC-Microgrids Clusters

Shafiee, Qobad; Dragicevic, Tomislav; Andrade, Fabio ; Vasquez, Juan Carlos; Guerrero, Josep M.

*Published in:*
Proceedings of the 40th Annual Conference of IEEE Industrial Electronics Society, IECON 2014

*DOI (link to publication from Publisher):*
10.1109/IECON.2014.7048785

*Publication date:*
2014

*Document Version*
Early version, also known as pre-print

# Distributed Consensus-Based Control of Multiple DC-Microgrids Clusters

Qobad Shafiee*, Tomislav Dragicevic*, Fabio Andrade†, Juan C. Vasquez*, Josep M. Guerrero*
*Institute of Energy Technology, Aalborg University (AAU), Aalborg, Denmark
Emails: qsh, tdr, juq, joz@et.aau.dk
† MCIA Innovation Electronics, Technical University of Catalonia, Barcelona, Spain
Email: fabio.andrade@mcia.upc.edu

***Abstract*—This paper presents consensus-based distributed control strategies for voltage regulation and power flow control of dc microgrid (MG) clusters. In the proposed strategy, primary level of control is used to regulate the common bus voltage inside each MG locally. An SOC-based adaptive droop method is introduced for this level which determines droop coefficient automatically, thus equalizing SOC of batteries inside each MG. In the secondary level, a distributed consensus based voltage control strategy is proposed to eliminate the average voltage deviation while guaranteeing proper regulation of power flow among the MGs. Using the consensus protocol, the global information can be accurately shared in a distributed way. This allows the power flow control to be achieved at the same time as it can be accomplished only at the cost of having the voltage differences inside the system. Similarly, a consensus-based cooperative algorithm is employed at this stage to define appropriate reference for power flow between MGs according to their local SOCs. The effectiveness of proposed control scheme is verified through detailed hardware-in-the-loop (HIL) simulations.**

***Index Terms*—DC microgrid clusters, droop control, distributed control, consensus protocol, voltage control, power flow control.**

## I. Introduction

DC microgrid (MG) is an effective solution to integrate modern electronic loads and alternative energy sources with dc output type such as photovoltaic (PV) systems, fuel cells, and energy storage systems [1]–[6]. In these systems, a more realistic scenario to achieve a higher quality of service and to enhance reliability is interconnection of several sources inside the MG or MGs together through the use of low-bandwidth communication (LBC) interface on upper control layers. Using the communication interface, dc MG will be able to employ higher control levels such as secondary, tertiary or supervisory control on the top of primary one.

Due to disbalance between power consumption and production, primary control introduces deviation of the common dc bus voltage. Therefore, a centralized voltage secondary control is implemented conventionally in order to restore the voltage (and frequency in the case of ac MGs) of the system to the nominal value. The secondary output signal changes the voltage reference of droop unit(s) accordingly by shifting the droop line up and down. This control loop could be also implemented in a distributed way over the MG units to avoid having a single point of failure [7]–[9].

On the other hand, in the case of connecting the MG to the other dc MGs or another dc bus, another control loop must be employed to control the power/current flow between them [10]. As power flow control can be accomplished only at the cost of having the voltage deviation inside the system, the centralized secondary control action could disable this feature. To cope with this, an alternative is to operate the upper control loops in distributed way.

Distributed averaging algorithms [11], [12] are well known as scalable and robust approaches where a series of local exchanges among neighboring units ultimately yield the same global average at every unit. The usage of these algorithms for MG application has been considered recently [8], [13]–[15]. A broadcast gossip algorithm is presented in [8] for secondary voltage and frequency control of ac MGs which tightly couples the communication and control layers. Consensus protocol based multi-agent schemes have been introduced for different purposes such as load restoration [15], fault recovery [13] and cooperative frequency control [14] of MGs.

In this paper, cooperative algorithms are utilized for hierarchical control of dc Microgrid clusters. In the primary level which is locally implemented, dc bus voltage is regulated and current sharing between the MGs sources can be achieved in a decentralized way. To improve efficiency of parallel batteries inside MGs, an adaptive droop method is presented in the primary level which defines droop coefficient automatically according to SOC of batteries. In the upper level, a distributed voltage control based on dynamic consensus protocol is proposed so that it will be able to regulate the bus voltage around the nominal value while respecting power flow control. Distributed power flow controller is added to regulate the tie-line current between the MGs. In this controller, a cooperative policy is utilized to determine the reference for the power flow control according to local SOC of batteries inside each MG.

The rest of the paper is organized as follows: Section II reviews primary control for dc Microgrids and introduces the adaptive droop control method. Section III presents a preliminary review of graph theory and consensus protocol. The distributed voltage regulator is proposed in Section IV. Section V introduces the cooperative power flow control. Performance of the control strategies is studied on a dc Microgrid clusters test system, where the results are reported in Section VI. Section VII concludes the paper.

## II. Primary Control

Primary control is employed locally for every source inside the MG in order to control the current injection into the common bus automatically. This level of control is generally made of inner control loops and droop control, as shown in Fig. 1. However, different control strategies can be used in the primary loop depending on the type of source in the MG [4].

Inner control loops are deployed as a first step of control based on direct measurements in order to regulate the voltage and current while maintaining the system stable. These loops comprise two control loops in general; the outer one is responsible for producing current reference and the inner one regulates the output current to follow that reference. Depending on the type of source inside the MG and the condition it has, the outer loop could have different forms such as maximum power point tracking (MPPT) mode for RESs, charging control strategy for ESSs, and voltage control loop. A RES operating in MPPT mode, behaves as current source converter (CSC) as it gives a constant current reference to the inner current loop. Similarly, batteries in regulated charging mode act as a CSC as they extract a constant power in any condition. In addition, RESs in MPPT mode and batteries when regulated charging act as a constant power source (CPS) and constant power load (CPL) respectively. Normally, the voltage and current loops employ proportional-integral (PI) regulators since they are easy to be implemented.

As control of dc bus voltage is a priority in the MGs, some of the units must operate in VSC. An outer loop called droop control is normally employed to be added to the inner control loops for parallel connection of these VSCs inside the MG.

### A. Conventional Droop Control

In dc MGs, a virtual output resistance loop representing droop control is implemented on the top of inner loops in order to connect a number of sources in parallel thus sharing load current between the units. In this case, a proportional part of the output current is subtracted from the output voltage reference of each MG unit to generate a reference for the inner voltage loop. This virtual loop will reduce the circulating current produced by physical differences between converters and lines. [5]. This control loop creates appropriate reference for the voltage inner loop as follows

$$v_{ref} = v^*_{MG} - R_d \cdot i_o \tag{1}$$

with $v^*_{MG}$ being MG voltage reference, $i_o$ is the output current and $R_d$ is the virtual resistance. The value of virtual resistance at different MG units determines how power is shared among them. Low value of $R_d$ must be used to ensure low voltage deviation in the dc bus. The larger droop gain is, the more voltage deviation and the more accurate is load sharing between the sources. In addition, instability of MG is more likely with the small value of $R_d$. Therefore, the droop method has an inherent trade-off between stability, voltage regulation and load sharing, and all of them should be taken into account when designing the virtual loop.

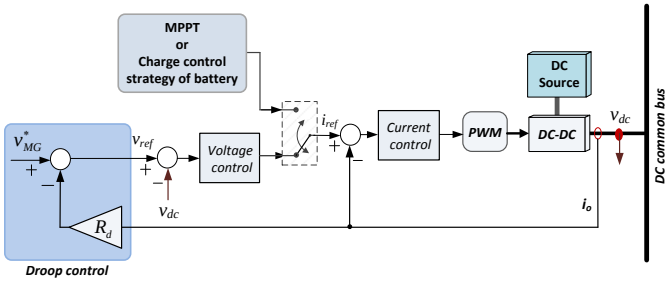


Fig. 1. Primary control of DC MGs.

Although in conventional method a fixed droop coefficient can be defined according to the ratings of individual converter, sometimes is needed to share currents in different ways. An adaptive droop scheme is described in the next subsection to share the currents based on SOC of batteries and thus equalizing local SOCs.

### B. Adaptive Droop Control

In islanded MG systems, batteries mostly operate in droop control mode as they are able to handle the power difference between RES production and load consumption automatically. In such systems, it is preferred participating in power sharing according to their SOCs [3], [4], since SOC equalization can be achieved among connected batteries. This way, life-cycle of batteries may improve as the batteries with small depth of charge are expected to have better life-cycle [16]. As discussed later in Section V, equalized local SOC of batteries is used in order to determine reference for control of current flow between interconnected MGs.

Adaptive droop methods have been addressed in some works recently [3], [4], [17]. An adaptive droop scheme is proposed for multi-terminal dc grids in [17] to share the load according to the available headroom of each converter and its impact on the stability of system has been investigated. In [3], a SOC dependent function is introduced only for discharging mode of ESSs inside a MG, while two separate functions have been presented for both charging and discharging mode of battery according to its capacity and the SOC [4]. A new adaptive droop function is described here which would be faster and more flexible than one presented in [4].

In order to equalize the SOCs in a general MG system, a battery with higher SOC should have dominant contribution in power sharing thus discharging at the most quick rate whereas the ones with lower SOC should be discharged with slowest rate participating lesser in the load sharing. The strategy is in contrary for charging mode. Moreover, battery capacity is also taken into account as it is inversely proportional to the changing rate of SOC. Therefore, droop coefficients are computed for charge and discharge conditions separately as follows:

$$\begin{cases} R^i_{d,\,charge} = \frac{C_i}{C_{\max}} \cdot \alpha \cdot (\frac{100}{100 - SOC_i})^k \\ R^i_{d,\,discharge} = \frac{C_i}{C_{\max}} \cdot \alpha \cdot (\frac{100}{SOC_i})^k \end{cases} \tag{2}$$

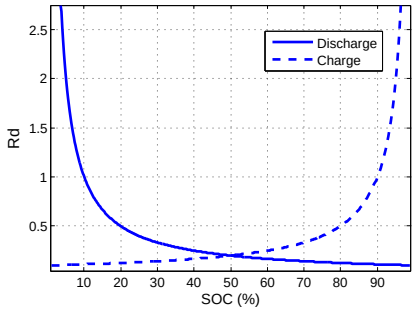


Fig. 2. Proposed charge and discharge functions for adapting the droop coeficient.

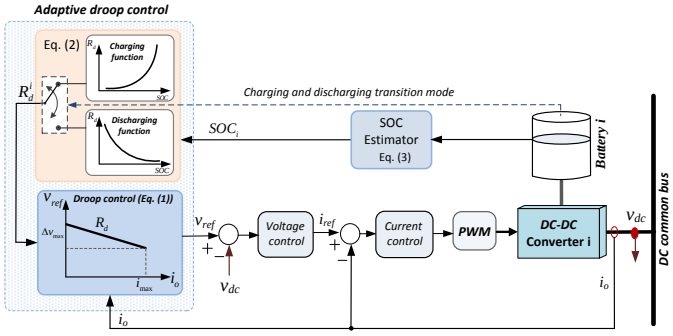


Fig. 3. Control diagram of the proposed adaptive droop control scheme for the $i$th connected battery to the MG.

where $C_i$ is the nominal capacity of battery $i$, $C_{\max}$ is the capacity of the battery with highest nominal capacity in the system, $k$ and $\alpha$ are user defined positive constants which determine the SOC-balancing speed and minimum value of droop coefficient, respectively. The higher $R_d$ the lower charge/discharge rate and vice versa.

Relationship between droop coefficient and SOC, presented in (2), is indicated in Fig. 2 for $k = 1$ and $\alpha = 0.1$. It is shown that higher $R_d$ is given to the battery with higher SOC when batteries are charging and when discharging, is allocated to one with lower SOC. Moreover, as it can be observed, $R_d$ is changed dramatically at the end (beginning) of charging (discharging) mode for small variation of SOC which results in faster charge/discharge rate. The speed of this rate, which is proportional to power sharing speed, is adjusted by changing the exponent $k$ while the minimum value of $R_d$ is defined by $\alpha$. Nevertheless, some limitation must be taken into account while defining these parameters with respect to the maximum value of dc voltage deviation, power sharing accuracy, stability issues and the power rating of each converter.

There exist several advanced methods to estimate SOC [18], [19]. Here we use ampere counting method which describes as follows

$$SOC_i(t) = SOC_i(0) - \frac{\eta_i}{C_i}\int_0^t I_i(\tau)\,d\tau \qquad (3)$$

where $I_i$ is battery current, $\eta_i$ is charging/discharging efficiency, and $SOC_i(0)$ is initial SOC. Control diagram of the proposed adaptive droop scheme for a connected battery inside a MG is shown in Fig. 3.

Simulation results showing implementation of proposed adaptive droop method on two parallel batteries inside a MG are presented in the following figures. The MG includes two batteries and two RESs supporting some loads. The capacity of batteries is considered to be 0.05 Ah to speed up the simulations.

The waveforms of SOC and input/output power of each converter are indicated in Fig. 4 and Fig. 5, for the proposed charging and discharging function of adaptive droop respectively, when $k = 2$ and $\alpha = 0.01$. As shown, in both modes, the battery with higher SOC absorbs/delivers more power than the one with lower. As a result, SOCs trends to be equalized,

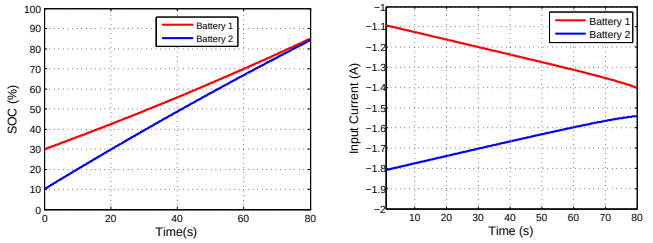


(a) (b)

Fig. 4. Performance of the proposed adaptive droop control in charging mode. (a) SOC1 and SOC2. (b) Input current of batteries.

while sharing the total power. Small signal stability analysis of the proposed method for different parameters, e.g., $k$, $\alpha$, and $SOC$, can be studied using the developed model by the authors in [20].

## III. Graph Theory and Consensus Protocol

We consider a network of communication links consisting of a set of nodes $V = \{v_1, v_2, ..., v_N\}$ connected through a set of edges $E = V \times V$, where $N$ is number of nodes. Such a network can be represented by a graph $G = (V, E)$. Each node is assigned with a MG in the cluster, and edges represent communication links for data exchange. Each node can only communicate with its direct neighbors. The communication graph does not require having the same topology as the underlying physical MGs. A matrix called adjacency matrix $A = [a_{ij}]$ is associated to the edges. $a_{ij}$ represents the weight for information exchanged between agents $i$ and $j$,

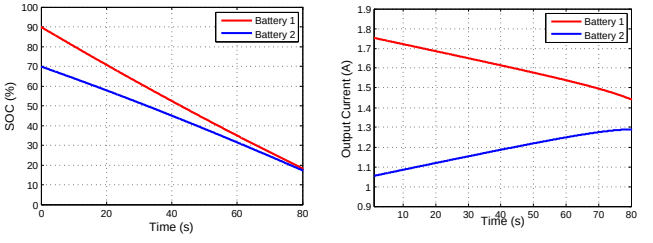


(a) (b)

Fig. 5. Performance of the proposed adaptive droop control in discharging mode. (a) SOC1 and SOC2. (b) Output current of batteries.

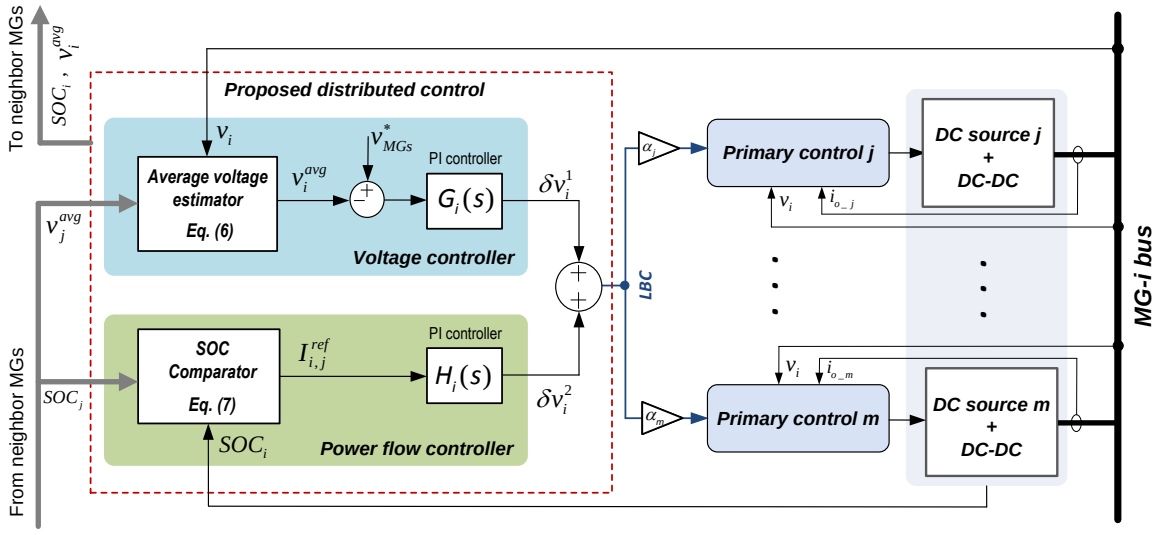


Fig. 6. Proposed hierarchical control for multiple DC microgrid clusters.

where $a_{ij} > 0$ if agents $i$ and $j$ are connected through an edge $(v_j, v_i) \in E$, otherwise, $a_{ij} = 0$. The set of neighbors of node $i$ is denoted $N_i$. Equivalently, if $j \in N_i$ , then $v_i$ receives information from $v_j$. However, the links are not necessarily bidirectional. If communication links are bidirectional, $(v_i, v_j) \in E \Rightarrow (v_j, v_i) \in E, \forall i, j$ the graph is said to be undirected, otherwise it is directed, and also termed a digraph. The laplacian matrix is defined as $L = D^{in} - A$, and its eigenvalues determine the global dynamics of the system. $D^{\text{in}} = \text{diag}\left\{d_i^{\text{in}}\right\}$, called in-degree matrix, is a diagonal matrix where $d_i^{\text{in}} = \sum_{j \in N_i} a_{ij}$. A graph is called balanced if the total weight of edges entering a node and leaving the same node are equal for all nodes [12]. A digraph is said to have a spanning tree if it contains a root node, from which there exists at least one direct path to every other node.

According to [12], a simple consensus algorithm to reach an agreement regarding continuous time integrator agents with dynamics $\dot{x}_i = u_i$ can be expressed as a distributed linear consensus protocol on a graph

$$\dot{x}_i(t) = \sum_{j \in N_i} a_{ij}(x_j(t) - x_i(t)) \tag{4}$$

The consensus value for protocol (4) can be, for instance, the average of the initial values, $(1/n)\sum_{i=1}^{n} x_i(0)$. Then, the collective dynamics of the group of agents can be written as

$$\dot{x} = -Lx \tag{5}$$

The convergence speed is determined based on laplacian matrix $(L)$ [12]. Thus, the weights need to be well designed in order to obtain faster convergence. For networks like power systems and Microgrids, $L$ can be designed to be symmetrical, i.e., $a_{ij} = a_{ji}$, in order to have plug-and-play and link failure resiliency features [21].

In this paper, different distributed policies are proposed to introduce two separate modules as discussed in the following sections; voltage regulator and power flow controller (see Fig. 6). The controllers are linked through a communication network. This communication network which is spanned across the cluster, enables data exchange among the controllers. Each controller e.g. controller at Node $i$, relays an information vector to its neighbors on the network. The information vector includes estimated average of voltage across the cluster ($v_i^{avg}$), and SOC of batteries inside MGs ($SOC_i$). Each controller receives data from its neighbors on graph and, after local processing of the information, it updates its control variables.

## IV. Distributed Voltage Control

A distributed voltage secondary control (DVSC) strategy is proposed here based on dynamic consensus protocol [22], in order to regulate the voltage in the MGs buses. As highlighted in Fig. 6, this voltage regulator provides a voltage correction term, $\delta v_i^1$, to be added to droop control units of $MG_i$, in order to restore the voltage at node $i$. Each controller uses dynamic consensus protocol to estimate the average of voltages across the cluster. The distributed protocol at each node (here Node $i$) is expressed as

$$\dot{v}_i^{avg}(t) = \sum_{j \in N_i} a_{ij}(v_j^{avg}(t) - v_i^{avg}(t)) + \dot{v}_i(t) \tag{6}$$

where $v_i$ is the measured voltage at Node $i$, $v_i^{avg}$ is the estimate of the average voltage provided by the estimator at Node $i$, and $v_j^{avg}$ is the estimation of voltage received from neighbor Node $j$. The estimated voltage is then compared with the reference voltage, $v_{MGs}^*$, which is normally the rated voltage of the MG, and fed to a PI controller, $G_i(s)$, to generate the voltage correction term, $\delta v_i^1$ (see Fig. 6).

Fig. 7 indicates implementation of the presented protocol in (6) for an arbitrary agent $i$. As seen in this figure, the local voltage, $v_i$, is used in the estimation process. This way, any voltage variation at any node, e.g., Node $i$, would immediately affect the estimation at that node, $v_i^{avg}$. It is shown in [22] that

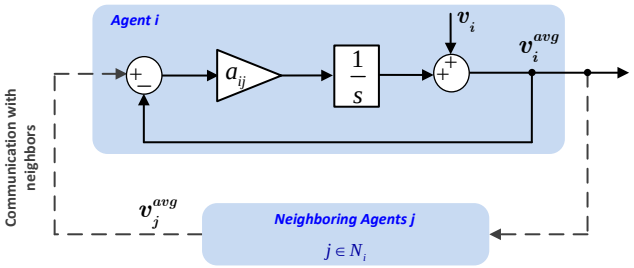


Fig. 7. Implementation of dynamic consensus protocol.

if the communication graph is balanced and contains at least a spanning tree, all estimations converge to a global consensus, which is the average value. Therefore, by choosing appropriate communication graph, all estimations will converge to the true average of voltages across the cluster.

The voltage regulator can operate in two ways; (i) centralized for the units inside each MG, termed as centralized voltage secondary control (CVSC), where it is able to remove voltage deviations inside each individual MG, thus providing smooth connection of MGs, (ii) distributed over the neighbor MGs when they are connected together to maintain MGs voltages around the reference. This way, the average voltage of all MG buses equals to the reference with an option to control current flow between the connected MGs.

## V. Distributed Power Flow Control

Once MGs are connected to each other (or to a stiff dc source), current/power flow between them requires to be managed. Power flow can be controlled by changing the level of voltage inside the MGs. To accomplish this goal, we propose a distributed power flow control (DPFC) over MGs so that each MG controls the tie-line with its neighbors according to a reference. As load profile or production of a MG might be changed, it is therefore not viable to use a predefined reference for current flow between MGs. It is felt by the authors that the best solution is to deploy SOC of batteries to define the reference, as it states the cumulative difference between production and consumption of the system. In order to apply this idea, in a cluster of MGs where each MG consists of arbitrary number of batteries, a MG with the highest average SOC should participate more in the current flow, injecting the highest current to its neighbors, while a MG with the lowest one absorbs the maximum current from the others.

The power flow controller at Node $i$, receives SOC of all its neighbors, e.g. the terms $SOC_j$ from all Nodes $j$, $j \in N_i$. Then it compares its SOC, $SOC_i$, with the weighted average of its neighbors' to calculate the SOC mismatch, $I_{ij}^{ref}$,

$$I_{ij}^{ref} = \sum_{j \in N_i} ba_{ij}(SOC_j - SOC_i) \tag{7}$$

where $b$ is the coupling gain between the voltage and power flow regulators, which determines the power flow control dynamics. This way we will be able to use the same communication infrastructure as for the voltage regulator. As seen in Fig. 6, the SOC mismatch, $I_{ij}^{ref}$, is passed through a PI

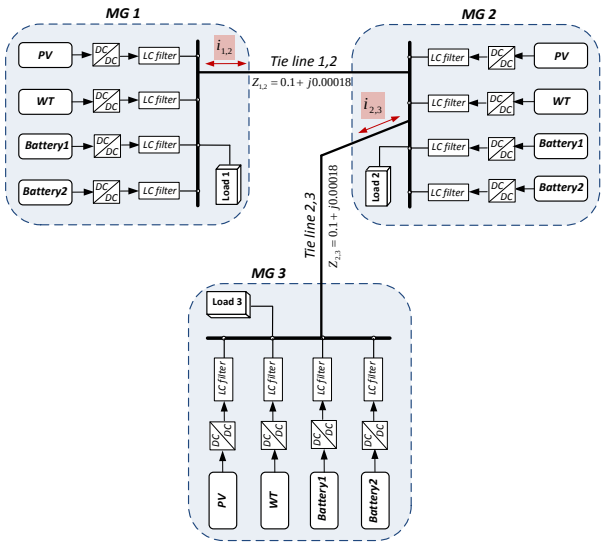


Fig. 8. HIL simulation case study: Three interconnected DC Microgrids.

controller, $H_i(s)$, to generate the second voltage correction term, $\delta v_i^2$ to be added to droop. This adjustment helps to lower the SOC mismatch among neighbors' MGs and, ultimately, make them all converge to the same value. Equivalently, the SOCs converge to a global consensus, and current/power will be regulated between the MGs accordingly.

It should be noted that the voltage correction terms, $\delta v_i^1$ and $\delta v_i^2$, must be limited, as large values might affect system stability. These correction terms can be also distributed along the sources inside each MG, passing through a participation factor ($\alpha$). Participation factor of batteries, for instance, can be according to their SOC and for RESs based on their power rate ($0 < \alpha \leq 1$).

## VI. Results

Hardware-in-the-loop (HIL) simulation results of three interconnected dc MGs, shown in Fig. 8, are presented here in order to show the feasibility of the proposed hierarchical control. In this case study, $MG_2$ is connected to $MG_1$ and $MG_3$ through resistive-inductive lines, and each MG consists of four units which are supporting some loads. PV and WT work in MPPT and two batteries work in droop controlled mode. For the simulation setup, the MGs voltage was selected at 48 V. Each MG can only communicate with its immediate neighbor, e.g. the one which is connected to it through electrical lines. The links are assumed bidirectional to feature a balanced Laplacian matrix. The proposed consensus algorithms and hierarchical control loops were developed in Matlab/Simulink. However, the final code was compiled into a dSPACE ds1006 platform in order to have HIL simulations. Electrical Setup and Control System Parameters are listed in Table I.

Fig. 9 shows a set of waveforms derived from implementation of proposed control scheme. In this figure, the voltage regulator is added to the all MGs in the first 2 s, and after connecting MGs, power flow control is activated in the second

TABLE I
ELECTRICAL SETUP AND CONTROL SYSTEM PARAMETERS

| Parameter | Symbol | Value |
|---|---|---|
| **Electrical parameters** | | |
| dc power supply | $Vin$ | 100 V |
| Input capacitance | $C$ | 2.2e-3 F |
| Converter inductances | $L$ | 1.8e-3 H |
| Inductor+switch loss resistance | $R_s$ | 0.2 Ω |
| Tie-line inductance | $L_t$ | 1.8e-3 mH |
| Tie-line resistance | $R_t$ | 0.1 Ω |
| Switching frequency | $f_{sw}$ | 10 kHz |
| **Primary Control** | | |
| Reference voltage | $v^*_{MG}$ | 48 V |
| Proportional current term | $k_{pi}$ | 5 |
| Integral current term | $k_{ii}$ | 560 |
| Proportional voltage term | $k_{pv}$ | 1.2 |
| Integral voltage term | $k_{iv}$ | 97 |
| Fixed droop coefficient | $R_d$ | 0.5 |
| **Voltage and Power flow control** | | |
| proportional voltage term | $k_{ps}$ | 0.1 |
| Integral voltage term | $k_{is}$ | 20 |
| proportional power flow term | $k_{pt}$ | 0.05 |
| Integral power flow term | $k_{it}$ | 10 |

half of operation. In the first scenario of simulation, only primary control operates inside the system and the MGs are disconnected having no current flow. In this period, different voltage deviations can be observed due to mismatch between production and consumption created by the droop control, since MGs are supporting different amount of loads, $20-$, $2-$, and $4-\Omega$ respectively; $MG_2$ injects about 22 A current which is approximately double of injected current by $MG_3$, while $MG_1$ feeds small amount of current, (see Fig. 9(b)). At $t = 2s$, the voltage regulator which is centralized for MGs individually, starts to act in order to restore the voltage deviations. As can be seen, it is able to eliminate steady state errors of bus voltages properly when MGs are not connected. Fig. 9(b) shows that MGs currents increase slightly, depending on the amount of deviation in each MG, in order to support the secondary control action.

In the second scenario, MGs are connected at $t = 3s$ and $t = 4s$, however, no current flows between them as there is no voltage difference in the MGs. As a result, one can conclude that connection of MGs could be quite smooth having no effect on the system stability, if we activate the voltage controller before connection. After activating the DPFC in the middle of simulation, current references produced by the proposed cooperative policy in 7, are imposed by this controller to be injected from $MG_1$ and $MG_3$ respectively, by producing some voltage deviation in the MGs buses (see Fig. 9(c)). At this moment, MGs currents changes accordingly as shown in Fig. 9(b) to follow the DPFC action. As can be observed, as soon as DPFC is added at $t = 6s$, voltage regulator becomes distributed in order to have current flow between the MGs. This way, DVSC maintains the MGs voltages around the acceptable range while DPFC controls the current flow according to the generated reference by the consensus algorithm.

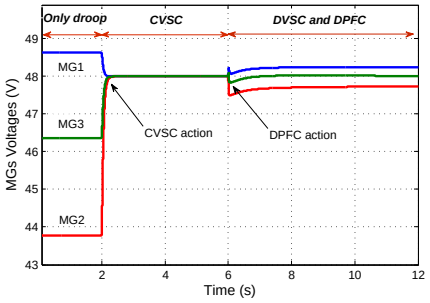


(a) microgrids voltages

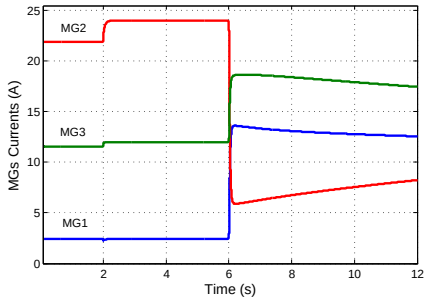


(b) microgrids currents

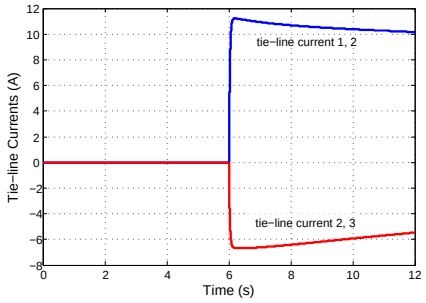


(c) Tie line currents

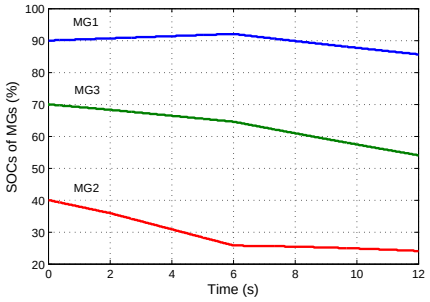


(d) SOCs of MGs

Fig. 9. Performance of proposed control methodology.

Fig. 9(d) represents total averaged SOCs of batteries in MGs for different scenarios. As this figure shows, the rate of charge/discharge changes when DPFC starts to act, as power/current reference is determined according to the SOCs; for instance $MG_1$ starts to be discharged with high rate while discharging rate of $MG_2$ decreases significantly. Moreover, the amount of tie-line currents get smaller as total SOCs of MGs trend to be equalized based on the proposed consensus

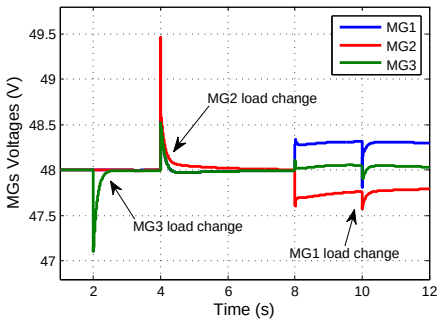


Fig. 10. Performance of the voltage regulator in rejecting load disturbances.

method. It is worth mentioning that SOC of batteries inside each MG is equalized using the adaptive droop method as explained in Section II.

Fig. 10 indicates the performance of proposed voltage control strategy in rejecting load disturbances ($50\%$ changes) inside the MGs before and after connection. MGs are connected at $t = 3s$ and $t = 3.5s$ respectively, and the distributed voltage regulator starts acting at $t = 8s$ as a result of activating the DPFC. The figure shows that the voltage control strategy is able to eliminate the load disturbances properly.

## VII. Conclusion

In this paper, distributed control schemes have been presented and tested for interconnected low-voltage DC microgrids. In the primary level, a SOC based adaptive droop function is proposed to define droop coefficient automatically, resulting in SOC equalization. A voltage controller is implemented for restoration of MGs voltage deviations. Using the centralized controller, power flow control is impossible to achieve when MGs are connected due to the fact that power flow is obtained at the expense of voltage deviations. To cope with this problem, dynamic average consensus algorithm has been utilized to make the voltage controller distributed when power flow control is required. Even though each agent (here each MG) may only communicate with its direct neighbors through a low-bandwidth communication, global information that is needed for distributed voltage control can be properly discovered by the proposed consensus˙based algorithm. Power flow control is implemented in order to control the tie-line currents between the MGs. To provide proper references for power flow control, a cooperative algorithm is proposed that uses total SOC of batteries inside the MGs. In this way, MGs trend to have equal SOCs despite of having different amount of loads. The control methodology uses a sparse communication network for data exchange. To verify the effectiveness of the proposed scheme, HIL simulation study is carried out.

## References

[1] H. Kakigano, Y. Miura, and T. Ise, "Low-voltage bipolar-type dc microgrid for super high quality distribution," *IEEE Trans. Power Electron.*, vol. 25, no. 12, pp. 3066–3075, Dec 2010.

[2] S. Anand, B. G. Fernandes, and M. Guerrero, "Distributed control to ensure proportional load sharing and improve voltage regulation in low-voltage dc microgrids," *IEEE Trans. Power Electron.*, vol. 28, no. 4, pp. 1900–1913, April 2013.

[3] X. Lu, J. M. Guerrero, K. Sun, and J. C. Vasquez, "An improved droop control method for dc microgrids based on low bandwidth communication with dc bus voltage restoration and enhanced current sharing accuracy," *IEEE Trans. Power Electron.*, vol. 29, no. 4, pp. 1800–1812, April 2014.

[4] T. Dragicevic, J. M. Guerrero, J. C. Vasquez, and D. Skrlec, "Supervisory control of an adaptive-droop regulated dc microgrid with battery management capability," *IEEE Trans. Power Electron.*, vol. 29, no. 2, pp. 695–706, Feb 2014.

[5] J. M. Guerrero, M. Chandorkar, T. Lee, and P. C. Loh, "Advanced control architectures for intelligent microgrids—part I: Decentralized and hierarchical control," *IEEE Trans. Ind. Electron.*, vol. 60, no. 4, pp. 1254–1262, April 2013.

[6] X. Lu, K. Sun, J. M. Guerrero, J. C. Vasquez, and L. Huang, "State-of-charge balance using adaptive droop control for distributed energy storage systems in dc microgrid applications," *IEEE Trans. Ind. Electron.*, vol. 61, no. 6, pp. 2804–2815, June 2014.

[7] Q. Shafiee, J. M. Guerrero, and J. C. Vasquez, "Distributed secondary control for islanded microgrids–a novel approach," *IEEE Trans. Power Electron.*, vol. 29, no. 2, pp. 1018–1031, Feb 2014.

[8] Q. Shafiee, C. Stefanovic, T. Dragicevic, P. Popovski, J. C. Vasquez, and J. M. Guerrero, "Robust networked control scheme for distributed secondary control of islanded microgrids," *IEEE Trans. Ind. Electron.*, vol. 61, no. 10, pp. 5363–5374, Oct 2014.

[9] A. Bidram, A. Davoudi, F. L. Lewis, and Z. Qu, "Secondary control of microgrids based on distributed cooperative control of multi-agent systems," *IET Gener., Trans. Dis.*, vol. 7, no. 8, pp. 822–831, Aug 2013.

[10] Q. Shafiee, T. Dragicevic, J. C. Vasquez, and J. M. Guerrero, "Hierarchical control for multiple dc-microgrids clusters," in *Proc. 11th intern. Multi-Conf. Syst. Signals Devices (SSD14)*, Feb 2014, pp. 1–6.

[11] T. C. Aysal, M. E. Yildiz, A. D. Sarwate, and A. Scaglione, "Broadcast gossip algorithms for consensus," *IEEE Trans. Signal Process.*, vol. 57, no. 7, pp. 2748–2761, July 2009.

[12] R. Olfati-Saber, J. A. Fax, and R. M. Murray, "Consensus and cooperation in networked multi-agent systems," *Proceedings of the IEEE*, vol. 95, no. 1, pp. 215–233, Jan 2007.

[13] H. Liang, B. J. Choi, W. Zhuang, X. Shen, A. S. A. Awad, and A. Abdr, "Multiagent coordination in microgrids via wireless networks," *IEEE Wireless Commun.*, vol. 19, no. 3, pp. 14–22, June 2012.

[14] W. Liu, W. Gu, W. Sheng, X. Meng, Z. Wu, and W. Chen, "Decentralized multi-agent system-based cooperative frequency control for autonomous microgrids with communication constraints," *EEE Trans. Sustain. Energy*, vol. 5, no. 2, pp. 446–456, April 2014.

[15] Y. Xu and W. Liu, "Novel multiagent based load restoration algorithm for microgrids," *IEEE Trans. Smart Grid*, vol. 2, no. 1, pp. 152–161, March 2011.

[16] T. David Linden, *Handbook of Batteries*, McGraw Hill, 2002.

[17] N. R. Chaudhuri and B. Chaudhuri, "Adaptive droop control for effective power sharing in multi-terminal dc (MTDC) grids," *IEEE Trans. Power Syst.*, vol. 28, no. 1, pp. 21–29, Feb 2013.

[18] M. Charkhgard and M. Farrokhi, "State-of-charge estimation for lithium-ion batteries using neural networks and ekf," *IEEE Trans. Ind. Electron.*, vol. 57, no. 12, pp. 4178–4187, Dec 2010.

[19] T. Dragicevic, S. Sucic, and J. M. Guerrero, "Battery state-of-charge and parameter estimation algorithm based on kalman filter," in *Proc. IEEE EUROCON*, July 2013, pp. 1519–1525.

[20] Q. Shafiee, T. Dragicevic, J. C. Vasquez, and J. M. Guerrero, "Modeling, stability analysis and active stabilization of multiple dc-microgrids clusters," in *Proc. IEEE Intern. Energy Conf. (EnergyCon14)*, March 2014, pp. 1–6.

[21] V. Nasirian, S. Moayedi, A. Davoudi, and F. L. Lewis, "Distributed cooperative control of dc microgrids," *IEEE Trans. Power Electron.*, vol. PP, no. 99, pp. 1–1, 2014.

[22] D. P. Spanos, R. Olfati-Saber, and R. M. Murray, "Dynamic consensus for mobile networks," in *Proc. 16th Int. Fed. Aut. Control (IFAC)*, 2005, pp. 1–6.